

# **Laser Offset Stabilization for Broadly Tunable TeraHertz (THz) Frequency Generation**

(Thesis submitted in partial fulfillment for the degree of Bachelor of Science)

Kevin Cossel

Mentor: Geoffrey Blake





**Table of Contents**

ABSTRACT .....	4
1. INTRODUCTION .....	5
1.1 <i>Terahertz Spectroscopy</i> .....	5
1.2 <i>Laser Stabilization</i> .....	7
1.3 <i>Optical-heterodyne sources</i> .....	10
1.4 <i>Terahertz offset frequency generation</i> .....	11
2. EXPERIMENTAL .....	12
2.1 <i>Frequency modulation spectroscopy</i> .....	12
2.2 <i>Proportional-integral-derivative (PID) Lock</i> .....	13
2.3 <i>Difference generation</i> .....	15
3. RESULTS .....	16
4. ANALYSIS .....	20
5. FUTURE WORK .....	24
6. CONCLUSION .....	26
REFERENCES .....	28

***Figures and Tables***

FIGURE 1: BLOCK DIAGRAM OF FREQUENCY MODULATION SPECTROSCOPY SETUP.....	12
FIGURE 2: PID FEEDBACK SCHEMATIC.....	14
FIGURE 3: THREE-LASER SETUP FOR PRODUCING TUNABLE TERAHERTZ RADIATION.....	15
FIGURE 4: SCHEMATIC OF OFFSET LOCKING METHOD.....	16
FIGURE 5: PID LOCKING RESULTS.....	17
TABLE 1: COMPARISON OF LOCKING PERFORMANCE .....	18
FIGURE 6: DIFFERENCE BETWEEN LASERS 1 AND 2.....	19
FIGURE 7: OFFSET LOCKING.....	20
FIGURE 8: HDO SPECTRUM FROM 1543-1544 NM.....	21
TABLE 2: PRIMARY LINE POSITIONS FOR HDO AND FREQUENCY DIFFERENCES BETWEEN ADJACENT LINES.....	23
FIGURE 9: EXTENDING THE OFFSET LOCKING CAPABILITIES TO 40 GHZ.....	24

**Abstract**

Spectroscopy and imaging in the terahertz region promises to be useful for a wide variety of applications. For remote sensing, terahertz spectroscopy could help in the identification of explosives and narcotics. In astronomy, terahertz imaging should provide new information about the composition of the interstellar medium and about the processes by which stars and planets are born. In chemistry and molecular biology, terahertz spectroscopy provides new rotational or rovibrational spectra of molecules and is useful in the study of hydrogen-bound clusters that serve as model systems for the quantitative understanding of the intermolecular forces involved in (bio)polymers and aqueous media. However, there are currently no terahertz sources that are easily tunable over the full region with high precision and accuracy. Here, we discuss the development of a novel three-laser source that allows for accurate stabilization of the difference frequency between two diode lasers to any frequency up to several terahertz, while still maintaining a long-term linewidth of under 10 MHz. When coupled with new traveling-wave photomixers, we will have a narrow linewidth, broadband terahertz source with high accuracy and capable of delivering up to tens of microwatts of power.

## 1. Introduction

There is a need for coherent sources of wide-bandwidth terahertz with high accuracy and narrow linewidth. Such a source would enable unprecedented research in the terahertz region with applications ranging from molecular biology to remote sensing to astronomy. We are developing a THz source based on optical-heterodyne conversion using new ultrahigh-speed photomixers that should provide at least  $10 \mu\text{W}$  of broadly tunable THz radiation. In this project, we developed the input source for the photomixer. In particular, we wanted to demonstrate the use of diode lasers to produce a tunable difference frequency with

- Multi-terahertz bandwidth
- Accurate to within 500 kHz
- High stability
- Linewidth of less than 10 MHz.

### 1.1 Terahertz Spectroscopy

The terahertz (THz) region, also known as the far-infrared (FIR) or sub-millimeter region, extends from about 0.1 to  $10 \times 10^{12}$  Hz, i.e., from 100 GHz to 10 THz ( $3 - 300 \text{ cm}^{-1}$ ,  $3000 - 30 \mu\text{m}$ ). This region is bracketed on the low-frequency end by the microwave region and on the high-frequency side by the infrared region.

In general, terahertz spectroscopy and imaging is useful for studying a variety of low-energy processes both in laboratory-based setups and for remote imaging. In the laboratory, terahertz radiation can be used to observe the pure rotational spectra of light molecules and the rovibrational spectra of heavier species. For example, terahertz studies are proving to be very useful in quantitatively characterizing the interactions in weakly bound clusters [1]. In fact, by using vibration-rotation-tunneling spectra over the full terahertz region it is possible to directly characterize the potential energy surface and related energy levels of clusters – information which has wide applications in chemical physics, theoretical chemistry, and molecular biology.

Another application of THz spectroscopy is remote sensing. Many materials are transparent to THz radiation, thus THz spectroscopy can be used to identify many chemicals such as explosives and narcotics. In space-based applications, sub-micron dust particles in the interstellar medium scatter visible and UV light. Thus, the dense clouds that harbor star formation cannot be studied using radiation at these wavelengths. Furthermore, the cooling caused by the scattering

of visible/UV photons results in temperatures around 10 K, which means that these objects radiate primarily at THz frequencies. With operations of the Stratospheric Observatory for Infrared Astronomy (SOFIA) imminent and the launch of the Herschel Space Telescope planned for 2008 the THz spectra of the interstellar medium can soon be studied in detail.

Because the spectral density of absorption lines in the THz region is expected to be much lower than that in the microwave region (due largely to excitation constraints and the Boltzmann Law), compound identification may well be much easier at THz frequencies. Thus, data from SOFIA and Herschel can be used to look for organic materials in the interstellar medium with very high sensitivity. However, searches of this type, as well as many other applications, require a laboratory-based THz spectrometer to first characterize the spectra of molecules of interest.

One major difficulty with studies in the terahertz region is the lack of very accurate and precise, yet broadly tunable radiation sources. In fact, the terahertz region has been nicknamed “the gap in the electromagnetic spectrum” [1]. At microwave frequencies, solid-state electronic oscillators can be used to produce high-power, tunable radiation; however, the power output dies off almost completely near 200 GHz. On the other hand, diode lasers can produce broadly tunable radiation throughout the infrared region, but at lower frequencies the long lifetimes associated with the spontaneous emission events prevent direct bandgap lasers from achieving inversion. New sources have been developed over the past 10 years; however, there is still no easily tunable source that covers the full THz range with high resolution. Backward wave oscillators, while easily tunable with high power output, do not cover the full frequency range and are large, expensive, and often have short lifetimes. Quantum cascade lasers have now lased to wavelengths as long as 140  $\mu$ m, and can produce nearly 10 mW of average power when operated at  $T < 10$  K [2]. Single mode operation of these devices is possible, but their tuning range is limited and the atomic layer control required in the fabrication of THz quantum cascade lasers has hindered their commercial availability (unlike the situation at infrared wavelengths).

An alternative technique, terahertz time domain spectroscopy, uses short sub-picosecond pulses, which are generated using dipole antenna radiators and a pulsed titanium-sapphire (Ti:Saph) or fiber laser, to probe a sample. Each frequency component is then detected by using a detector that is gated using an optical delay line and the pulsed Ti:Saph laser. While this system has wide bandwidth, it is fairly expensive and also of limited resolution (the resolution is limited by the delay line and the laser pulse width). The continuous wave (CW) implementation of such

techniques uses two lasers and is known as optical-heterodyne conversion. Potentially this approach can provide both exceptional tunability and frequency resolution; however, current systems [3-6] are not very stable and are difficult to tune.

We are working on developing a new, ultra-broadband source of terahertz radiation capable of very accurate frequency generation and spanning almost the entire terahertz region (i.e.,  $> 5$  THz of bandwidth). This will be accomplished by optical-heterodyne conversion using new erbium arsenide doped indium-gallium arsenide (ErAs/InGaAs) photomixers that radiate at the difference frequency between two input continuous wave lasers. These photomixers allow the use of diode lasers with wavelengths near 1550 nm, that is, within the telecommunications band. This allows us to take advantage of the continuing development in telecommunications technology, such as high-power, low-noise fiber amplifiers. The goal of this project was to develop the input source to the THz photomixer. To that end, we wanted to create a tunable offset of at least several THz between two stabilized  $\sim 1550$  nm diode lasers.

In order to obtain good line resolution, the linewidth of the probing radiation should be less than the width of the absorption lineshapes of interest. For water at 2.5 THz the Doppler-limited linewidth is around 7.5 MHz, thus we wanted to stabilize each laser to a few MHz. Here we discuss a technique that allows for wide bandwidth offset generation while still maintaining a laser beat note linewidth of 3 to 4 MHz and a frequency stability that is even better.

## 1.2 Laser Stabilization

Frequency modulation spectroscopy (FMS) is a standard high-sensitivity technique, which is often used in a feedback loop used to reduce the linewidth of diode lasers [7-17]. In its simplest form the frequency of the laser is modulated by changing the diode injection current sinusoidally. This modulation produces a laser beam with electric field

$$E(t) = E_0 \exp[i(\omega_0 t + M \sin(\omega_m t))],$$

where  $M$  is a parameter known as the modulation index [18]. In this form, the frequency is given by the time derivative of the phase, so the frequency varies about  $\omega_0$  (the laser frequency) by at most  $M\omega_m$ . This field can be represented by the Fourier series,

$$E(t) = E_0 \exp(\omega_0 t) \sum_{n=-\infty}^{n=\infty} J_n(M) \exp(in\omega_m t).$$

Here, the modulation is represented as sidebands with the amplitude of the  $n^{\text{th}}$  order sideband given by the  $n^{\text{th}}$  order Bessel function of  $M$ . In the case where  $M \leq 1$  (which is typical in most physical applications), all second order and higher sidebands are negligible and we have

$$E(t) \approx E_0 \exp(i\omega_0 t) \left( -\frac{M}{2} \exp(-i\frac{M}{2}\omega_m t) + \exp(i\omega_m t) + \frac{M}{2} \exp(i\frac{M}{2}\omega_m t) \right).$$

In particular, notice that the upper and lower sidebands are out of phase with each other due to the behavior of the Bessel function.

After the modulation is applied, the laser beam is directed through an absorption cell. We can represent the result of the absorbing sample as a frequency-dependent transmission function,

$$T(\omega) = \exp(-\delta - i\varphi),$$

where  $\delta$  is the absorption (intensity change) and  $\varphi$  is the dispersion (phase change). The output from the sample cell is now just  $E(t)$  with the intensity of each band scaled by  $T(\omega)$ .

The photodetector outputs a signal proportional to the intensity of the impinging electric field, that is, the output is proportional to

$$|E(t)^2| = E_0^2 \exp(-2\delta_0) [1 + 2M \cos(\omega_m t)(\delta_{-1} - \delta_1) + 2M \sin(\omega_m t)(\varphi_{-1} + \varphi_1 - 2\varphi_0)].$$

Using an RF double-balanced mixer we can phase-sensitively detect either the in-phase (cosine or absorption) spectrum or the quadrature (sine or dispersion) spectrum. In particular, notice that the absorption spectrum depends on the relative attenuations of the upper and lower sidebands.

A more qualitative understanding is obtained by considering the effect of sweeping the wavelength of a frequency-modulated beam across an absorption line. Far below the line neither sideband is attenuated, so the phase-detected signal is zero. This is because the beat signal between the upper sideband and the main band is canceled by the inverse beat signal between the lower sideband and the main band (since the lower sideband is out of phase and inverted with respect to the upper sideband). As the laser moves towards the absorption the upper sideband is more attenuated than the lower sideband, which leads to a negative signal. Once the upper sideband is past the absorption line center the signal begins to increase (becoming less negative) as the sideband becomes less attenuated. When the laser is tuned exactly to the center of the absorption both sidebands are attenuated by the same amount leading to zero signal. As the laser moves above the absorption line the lower sideband is now attenuated more than the upper sideband, so the observed signal is positive. Finally, far above the absorption line the signal is

again zero. Thus we see that the FM in-phase signal is just the first derivative of the absorption line (for small modulation depth).

The first derivative of an absorption line provides a very useful signal for laser frequency stabilization. Because the wavelength of diode lasers depends on a variety of factors including the diode temperature, supply current, and diffraction grating position (for grating stabilized lasers), the wavelength of diode lasers usually drifts and fluctuates over time. While this is fine if you want light near a certain wavelength, it is not good for precision applications. However, diode lasers are convenient light sources still because they are relatively inexpensive, long-lived, and tunable over a very broad range. For this reason, methods of stabilizing the wavelength of diode lasers and keeping the laser a certain wavelength with narrow linewidth are very important. The first derivative absorption line can be used as an error signal to lock the laser to the absorption line. At the absorption line center the error signal is zero while above the line the signal is positive and below the line the error signal is negative. By sending this signal to a device to control the laser wavelength (such as a current source, piezo control for the grating, or an acousto-optic frequency shifter) it is possible to lock to the absorption line – providing an absolute frequency reference that is insensitive to environmental conditions.

Just directly feeding back the error signal from FMS to the laser's wavelength control mechanism of the laser provides some correction for small errors; however, it is not robust enough to provide good locking. In particular, this method, known as proportional feedback, only helps to correct changes about the center position of the laser without feedback. If the center position of the laser moves or is not located exactly at the absorption line center, both of which are common situations for diode lasers, the laser is not locked to the absorption line center. A better feedback method uses a proportional-integral-derivative (PID) controller [7, 14]. The final output of an ideal PID controller is [19]

$$\text{Output}(t) = K_p e(t) + K_i \int_0^t e(t') dt' - K_d \frac{de}{dt}.$$

The output is still directly proportional to the error signal  $e(t)$  with the proportional gain given by  $K_p$ ; however, there are two more components to the feedback. The first is a term proportional to the integral of the error signal, which serves to keep the laser at the error signal null. If the laser begins to drift the integral of the error builds up and pushes the laser back to the zero point. The third term is proportional to the derivative of the error. This term helps to improve stability and

decrease overshoot by ‘anticipating the future.’ For example, if there is a sudden, large change the integral term reduces the output to prevent the system from over reacting to this change. PID loops can be implemented using analog electronics (e.g., with operational amplifier based integrators and differentiators), or digitally with software or a microcontroller. We chose to use analog controllers here because they are often faster than digital loops; however, a microcontroller or field-programmable gate array (FPGA) based loop may also have the speed desired and could provide a low noise, easily customizable system.

Since a laser stabilized using FMS is always stabilized to the center of the absorption line, the frequency of the laser can be used as a stable frequency reference throughout the experiment; however, the stability is also a possible disadvantage of FMS based stabilization. For example, if two lasers are stabilized to different absorption lines and then combined to produce a difference frequency, such as the terahertz frequency desired here, that frequency is not tunable. The only possible tunability derives from changing the locking lines, which does not provide fine control of the output frequency. Thus, a somewhat more complex system is needed in practice.

### 1.3 Optical-heterodyne sources

In some semiconductor materials, known as photoconductors, laser excitation leads to a photo-excitation of charge carriers and subsequent propagation through the material. If the laser (with frequency  $\nu$ ) strikes that active area with angle of incidence  $\theta$ , the resulting wave propagates along the conductor with propagation constant

$$k = \frac{2\pi\nu \sin(\theta)}{c}.$$

If two lasers with different frequencies are combined on the photomixer, an interference fringe pattern is produced. This fringe pattern oscillates at the difference frequency between the two lasers, that is  $\nu_{\text{fringe}} = (\nu_1 - \nu_2)$ . The interference pattern propagates with velocity

$$v = \frac{2\pi(\nu_1 - \nu_2)}{k_1 - k_2} = \frac{(\nu_1 - \nu_2)c}{\nu_1 \sin(\theta_1) - \nu_2 \sin(\theta_2)}.$$

This velocity can be tuned by varying the incidence angles of the two lasers [1, 3, 20-22].

If the interference pattern is coupled to an embedded dipole antenna, radiation is produced. The frequency of this radiation is just given by the frequency of oscillation of the photocarrier current, which in turn is just the difference frequency between the lasers. By varying the angle of incidence of the two lasers (to match the velocity of propagation with the group velocity of THz

waves), it is possible to generate coherent radiation of several  $\mu\text{W}$  power at THz difference frequencies. As described below, the first application of such a traveling wave photomixer used lasers near 850 nm and low temperature grown gallium-arsenide (LTG GaAs) as the photomixer material [5]. We are presently developing a next generation of photomixers based on ErAs/InGaAs that can be pumped at 1550 nm [23], where the ready availability of fiber amplifiers with 1-10 W output should enable the generation of THz output into the several tens of  $\mu\text{W}$  range.

#### 1.4 Terahertz offset frequency generation

We have developed a new technique using three diode lasers, each with wavelength near 1550 nm, which allows the difference between two lasers to be tuned over a multi-terahertz window. Furthermore, by stabilizing all three lasers, we can generate any difference frequency of interest with high accuracy and narrow linewidth. This combination of ultra-high bandwidth and narrow linewidth using 1550 nm lasers is unmatched by any existing system.

Previous optical-heterodyne based THz sources used LTG GaAs photomixers and 850 nm diode lasers locked to cesium atomic transitions or tunable Fabry-Perot cavities. Unfortunately, fiber lasers and amplifiers are not available at 850 nm, so the system must employ free-space optics rather than fiber coupling in order to combine the lasers before focusing onto the photomixer. Furthermore, because of the cavities and the optical coupling the overall system is not stable over long periods of time, is hard to set up, and is difficult to tune [3, 5]. Thus we used standard telecommunications band (1550 nm) fiber coupled diode lasers throughout this setup. The switch to 1550 nm was possible because of the recent development of ErAs/InGaAs photomixers that operate at this wavelength.

We use absorption lines of mono-deuterated water (HDO) to stabilize the lasers. However, just locking two lasers to different HDO lines does not provide the continuous tunability desired in a broadband source (the output is only step tunable by choosing different locking lines). Thus, we use a three-laser design. Narrow-range tunability is accomplished by offset locking the third laser to one of the other two lasers. In this arrangement the difference between one laser locked to an HDO line and another laser is stabilized to any frequency from 0 to  $\pm 40$  GHz. A third laser is then locked to a different HDO line. By changing the offset locking frequency and the absorption line to which the third laser is locked, the difference between two stabilized lasers can

be varied over many THz. When combined with optical-heterodyne generation, this allows for a broad-bandwidth, continuously tunable source of narrow linewidth radiation up to several THz.

## 2. Experimental

### 2.1 Frequency modulation spectroscopy

Fig. 1 shows our setup for frequency modulation spectroscopy of HDO. HDO was generated from a 1:1 solution of H<sub>2</sub>O and D<sub>2</sub>O. The sample cell was filled with ~ 20 torr of vapor from this solution by first evacuating the cell and then bleeding in vapor from above the liquid. This cell was used as a single-pass absorption cell with a path length of about 1m.

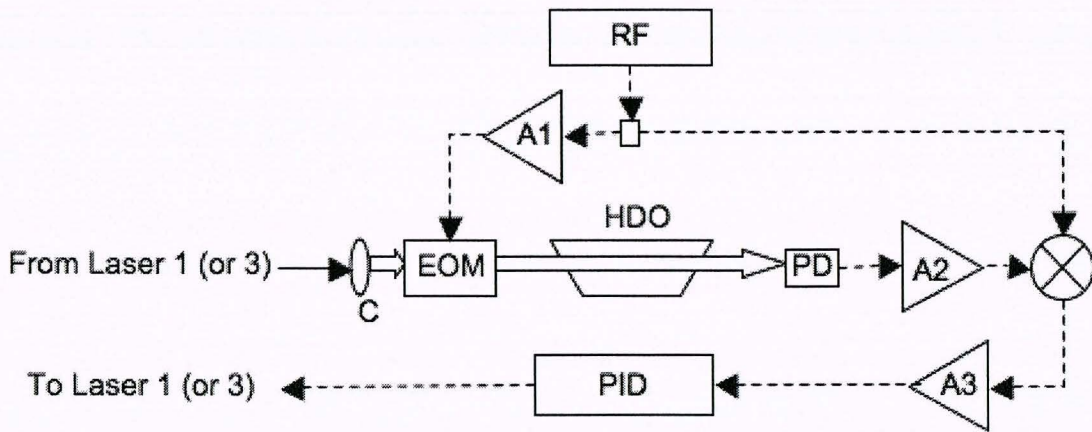


**Figure 1: Block diagram of frequency modulation spectroscopy setup.** FMS on HDO is used to provide the locking error signal to lasers 1 and 3. After passing through a collimating lens (C), an electro-optic modulator (EOM) provided laser frequency modulation. The modulated laser passed through an HDO cell and onto a high-speed photodetector (PD). The resulting signal was amplified (A2, wideband RF amplifier), down-converted, and then amplified again (A3, SRS 560 preamplifier). An RF source at 130 MHz and 17 dBm was used to drive both the EOM (after amplification) and the mixer.

Laser light was generated using a fiber-coupled Agilent 81640 tunable, external-cavity diode laser, which provided about 2 mW of output power that was split with a 50:50 coupler. Half of the output (1mW) was directed to a fiber collimator (OzOptics) for frequency stabilization, the other half is available for amplification and THz photomixing. After collimation the laser beam was directed through a free-space electro-optic phase modulator (EOM, resonant mode NovaPhase 4003) driven at 130 MHz with a power level of 26 dBm (into 50 ohms) to produce the necessary frequency modulation.

After passing through the absorption cell, the laser beam was detected with a 150 MHz InGaAs photodiode (ThorLabs PDA-10C). The output from the photodiode is the 130 MHz beat note between the sidebands, generated by the frequency modulation, and the center band. This beat note was then amplified and mixed with the 130 MHz EOM drive signal (at 14 dBm) using a Minicircuits ZWL-1H double-balanced mixer. This mixer serves as a down-converter and outputs a DC voltage corresponding to the amplitude of the beat note. Finally, the DC signal was filtered with a 100 kHz, 6dB low-pass filter and amplified by 500 with a SRS 560 preamplifier. The resulting error signal was used directly in the PID loop (described later) and also monitored with an analog-to-digital converter (the auxiliary input of an SRS 830 lock-in amplifier).

Using this setup we observed that, on a short (1 second) time frame, the error signal was actually photodetector noise limited, not laser noise limited. Larger scale changes due to laser instabilities were noticed over a longer time frame. This is not ideal because it means that the PID loop will not stabilize any rapid laser fluctuations but will only correct slower laser drift. In fact, the laser linewidth was observed to increase slightly on short time scales when the laser was locked because the photodetector noise was fed back into the laser. In an effort to increase the signal-to-noise ratio, we included a fiber amplifier before the collimator, which increased the laser power to 50 mW and allowed the gain on the SRS preamplifier to be reduced accordingly. This change shifted the noise to light-source limited and allowed the PID loop to slightly reduce the short-term linewidth; however, it is uncertain whether most of the light-source noise is laser related and how much is amplifier related. Significant additional improvements are planned to further increase the signal-to-noise ratio (see Further Work).

## 2.2 Proportional-integral-derivative (PID) Lock

Locking to the HDO line is accomplished using the home-built PID controller shown in Fig. 2. Block 1 provides a high-impedance buffer and allows for variable attenuation and offset of the error signal input. The error signal is then fed into Blocks 2, 3, and 4. Block 2 is a standard variable gain, inverting amplifier, while Block 3 is a standard differentiator. Block 4 is a precision integrator that allows resetting and holding. The outputs from these three blocks are fed, along with a buffered external input (to allow for tuning), into a summing amplifier/low-pass filter and output buffer. Most of the component values were based on previously reported systems [7, 14] and were then modified to obtain the best performance in this system. In particular, we changed the low-pass filter cutoff to increase the speed, increased the feedback

capacitor on the integrator to increase stability (prevent the integrator from acting too quickly), and increased the relative differential gain to reduce high-frequency laser noise.

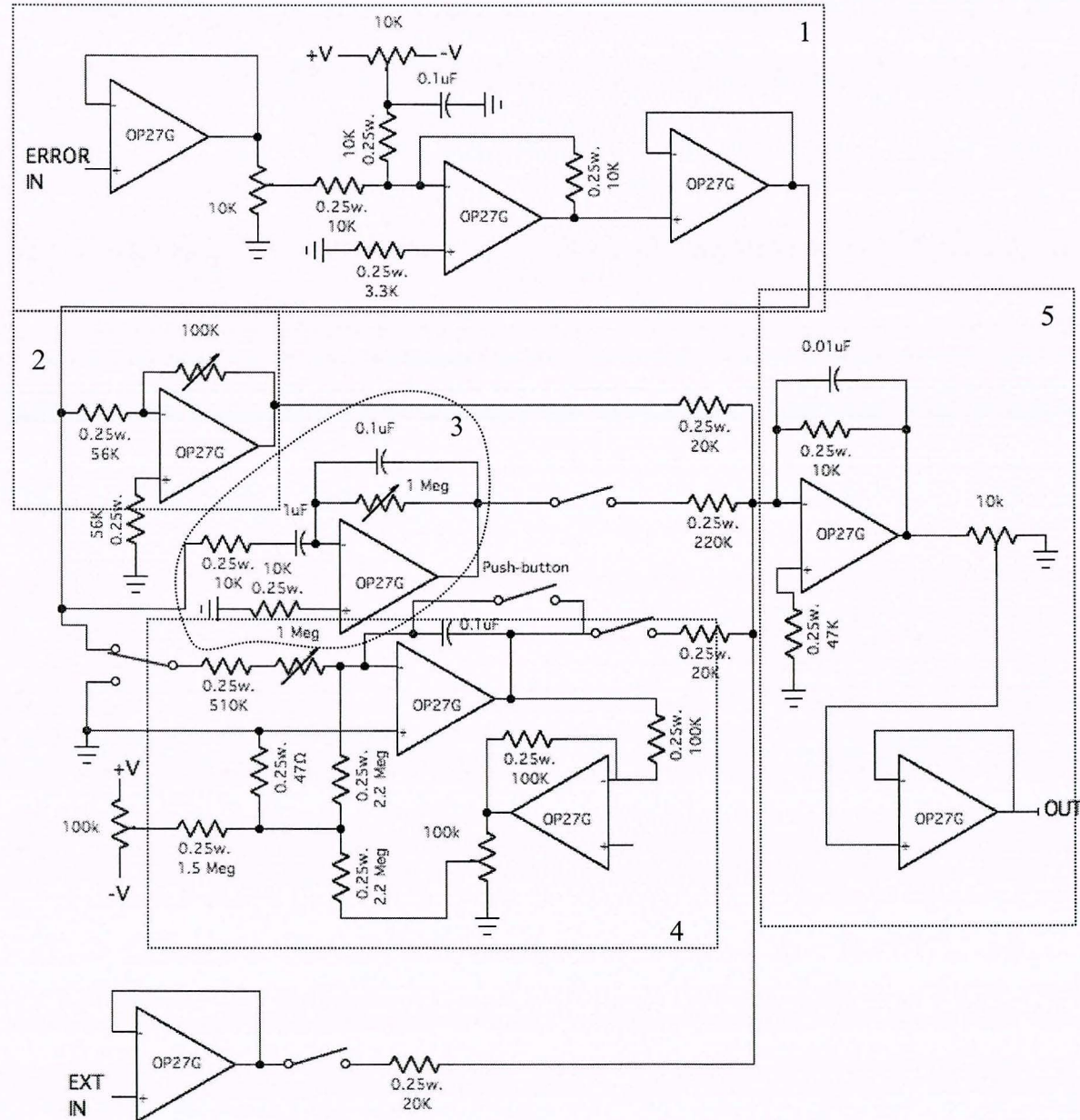


**Figure 2: PID Feedback Schematic.** The error signal is buffered, attenuated, offset, buffered again, and sent to an op-amp based proportional amplifier, differentiator, and precision integrator. Each of these outputs are added to an external input, then filtered and buffered.

### 2.3 Difference generation

We propose the novel three-laser source shown in Fig. 3 to generate a tunable offset between two lasers. Lasers 1 and 3 are both stabilized to different absorption lines of HDO using FMS. The lines are chosen such that the difference between them is within  $\pm 40$  GHz of the desired output frequency. Laser 2 is then offset locked to laser 1 by up to  $\pm 40$  GHz. Scanning can be accomplished by sweeping the offset from minimum to maximum, stepping Laser 3 to the next HDO line, and then repeating.

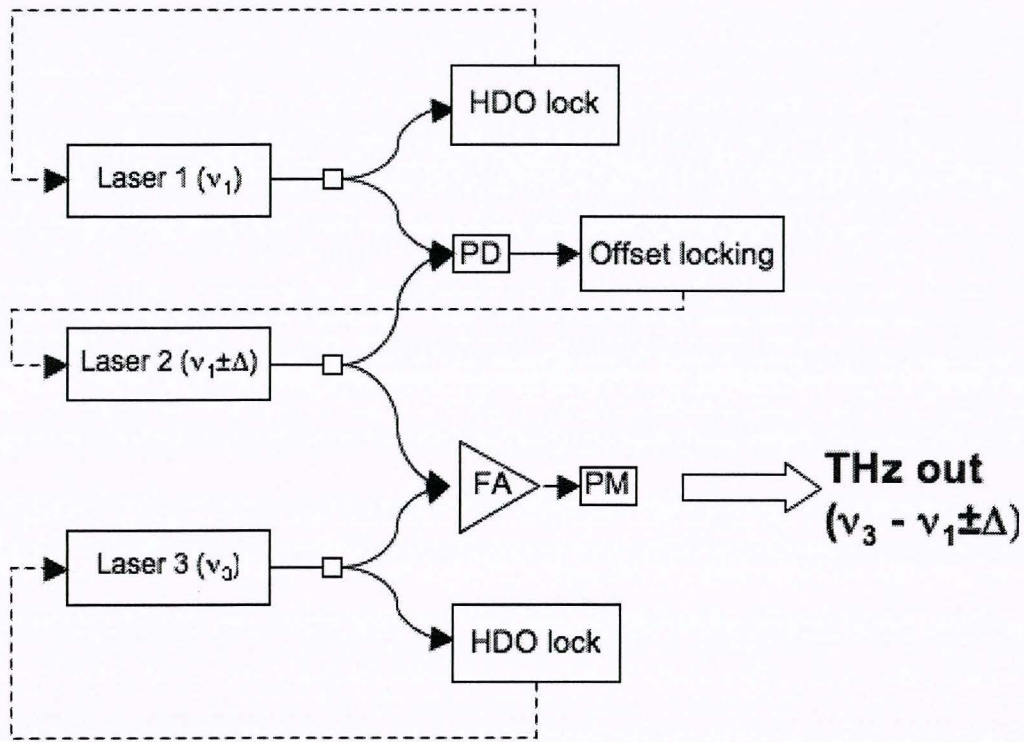


**Figure 3: Three-laser setup for producing tunable terahertz radiation.** In this setup, laser 1 and laser 3 are locked to two different HDO lines that are separated by the approximate frequency of the desired output. Fine-tuning is accomplished by offset locking laser 2 from laser 1 by  $\pm 40$  GHz. The final output is then obtained by combining lasers 2 and 3 on an ultra-high speed photomixer (PM) after amplification with a fiber amplifier (FA).

Fig. 4 shows the current setup for offset locking Laser 2. Light from Lasers 1 and 2 was combined using a fiber coupler and then impinged on a 40 GHz fiber-coupled photodetector (New Focus 4011), whose output is the beat note equal to the difference between Lasers 1 and 2. This signal was down-mixed with a Miteq triple-balanced 2-18 GHz mixer. The mixer local oscillator (LO) was supplied by a Wiltron tunable RF synthesizer, which is chosen so that the

intermediate frequency (IF) output is between 0.5 and 1 GHz. This IF was then locked to 600 MHz using a prescaler based source-locking microwave counter (EIP 578) by feeding back the coarse and fine locking outputs to Laser 2. Now, as the RF is varied, the frequency of Laser 2 changes as well.

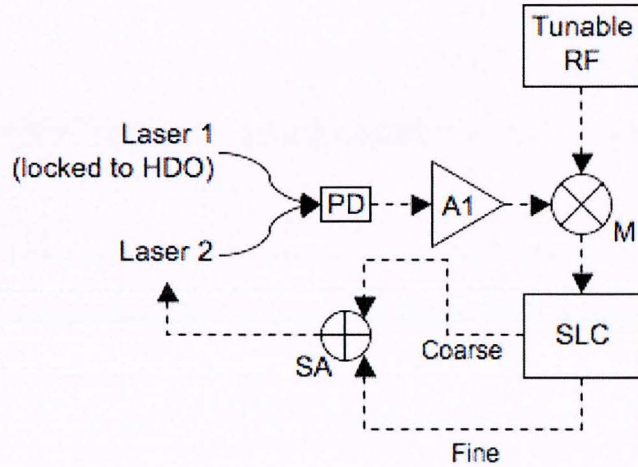


**Figure 4: Schematic of Offset Locking Method.** Light from Lasers 1 and 2 is sent to a 40 GHz photodetector (NewFocus). The output is amplified (A1, wideband, Miteq) and mixed with a tunable RF source (Wiltron 0.1-20 GHz, 16 dBm) with a triple-balanced mixer (M, 2-18 GHz, Miteq). The IF is then sent to an EIP source locking counter (SLC). The two lock outputs are combined with a summing amplifier (SA) and sent to Laser 2.

### 3. Results

Figs. 5-7 and Table 1 show the locking capabilities of the system. Over a two hour period (Fig. 5a), the error signal from the FMS setup showed a slow drift of >100 MHz deviation, plus significant higher frequency noise. On the other hand, the same laser locked to an HDO line with the PID loop shows deviations of 10 MHz peak-peak without any drift or large amplitude spikes. The PID loop reduced the standard deviation from 50 MHz to 3.5 MHz, with a mean accuracy of 20 kHz. Fig. 5b shows a 10 second time window. Again we see fluctuations of 30 MHz in the free-running laser (standard deviation of 5.5 MHz) whereas the PID stabilized laser showed 10 MHz peak-peak deviations and a standard deviation linewidth of just over 3 MHz.

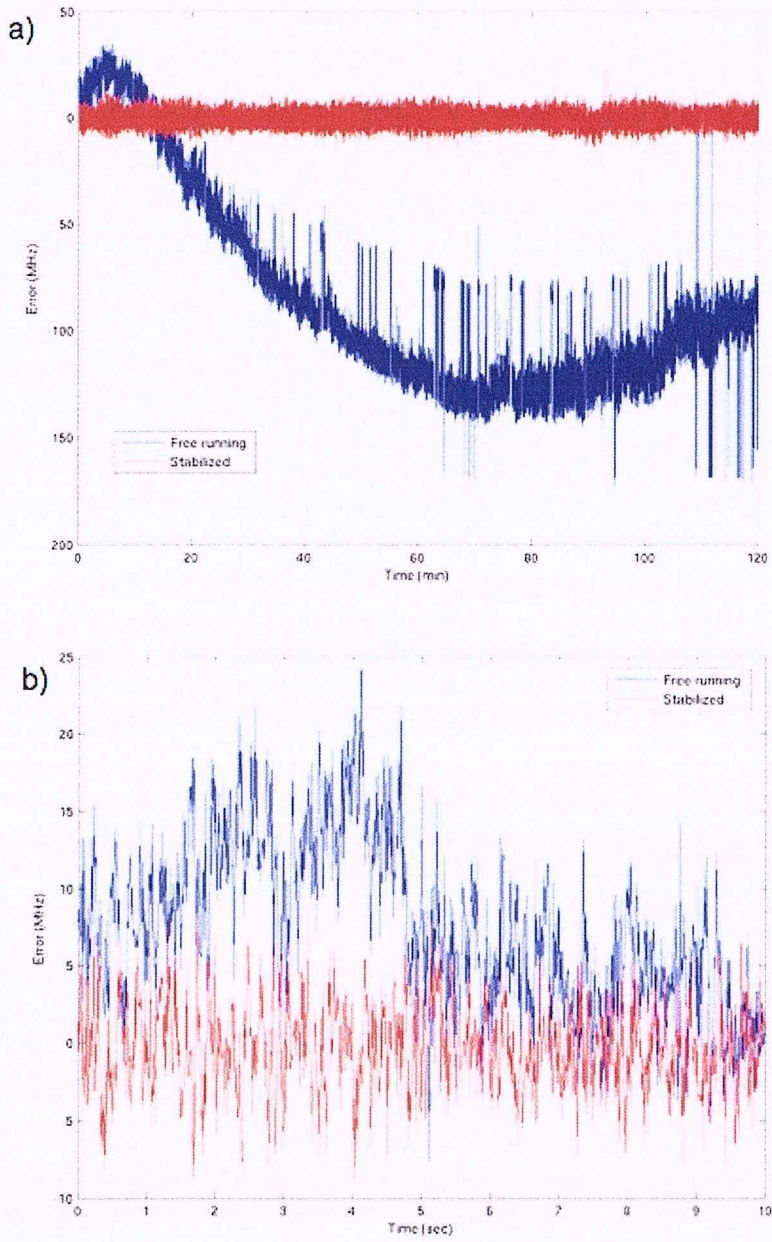


**Figure 5: PID Locking Results.** (a) The free-running laser (blue) showed considerable drift of 150-200 MHz over two hours while the PID stabilized laser (red) remained locked to within a few megahertz; (b) Over 10 seconds the free-running laser (blue) showed 30 MHz of deviation while the PID stabilized laser showed 10 MHz peak-peak fluctuations.

The difference frequency between Lasers 1 and 2 can be recorded directly from the source-locking counter. Fig. 6a shows the difference frequency between Lasers 1 and 2 with both lasers free-running (blue) and also with Laser 1 locked to an absorption line of HDO (red). Notice again that PID locking of Laser 1 significantly reduces drift. Using the source-locking counter,

Laser 2 can be offset locked from Laser 1. In Fig. 6b Laser 1 was locked to an HDO line and Laser 2 was offset locked from Laser 1 by 600 MHz. Offset locking the two lasers (without feedback from any HDO lines) considerably stabilizes the beat note to within 20 kHz of the set frequency (averaged over the acquisition time) and with a standard deviation of  $\sim 1$  MHz. Furthermore, this system remained locked for 15 hours, indicating a high degree of stability. By using a mixer to down-convert the photodetector output to an IF that could be read on the source-locking counter (Fig. 4), we were able to offset lock Laser 2 up to 20 GHz from Laser 1. Fig. 7 shows Laser 2 offset from Laser 1 by 13.6 GHz.

**Table 1: Comparison of locking performance**

	Mean (MHz)	Standard deviation (MHz)	RMSE (MHz)	Drift (MHz/s)
<b>Free-running<sup>1</sup></b>	<b>-83.3<sup>2</sup></b>	<b>47.5<sup>3</sup></b>	<b>4.87<sup>4</sup></b>	<b><math>\sim 2</math></b>
<b>PID stabilization<sup>5</sup></b>	<b>-0.0196</b>	<b>3.48</b>	<b>3.48</b>	<b>-5e-5<sup>6</sup></b>
<b>Offset locking<sup>7</sup></b>	<b>599.74</b>	<b>1.32</b>	<b>1.32</b>	<b>&lt; 1e-6</b>
<b>Stabilized THz output<sup>8</sup></b>	<b><math>\pm 0.3^9</math></b>	<b>7</b>	<b>9</b>	<b>&lt; 1e-4</b>

[1] Single laser  
[2] From error signal (Figure 5a)  
[3] Standard deviation over 2 hour collection window calculated from error signal (Figure 5a)  
[4] Fit difference frequency (Figure 6a) with quadratic. RMSE for one laser = RMSE/ $\sqrt{2}$   
[5] Laser 1 stabilized to HDO line (Figure 5a).  
[6] Slope of linear fit to data.  
[7] Data read from frequency counter (Figure 6b).  
[8] Estimated. This is the result of two PID stabilizations (on Lasers 1 and 3) and offset locking of Laser 2.  
[9] Accuracy.

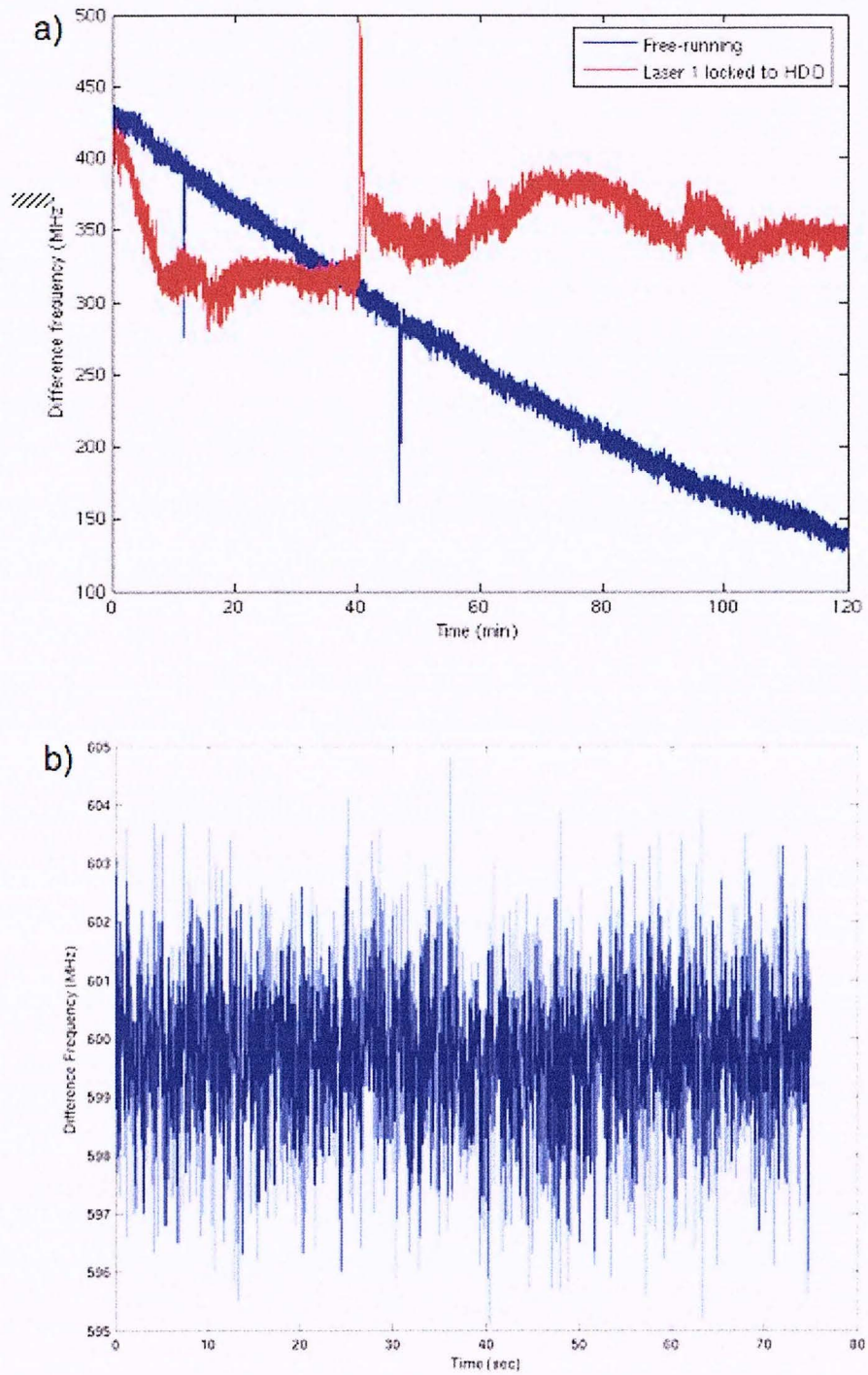


**Figure 6: Difference between Lasers 1 and 2.** (a) Difference frequency between Laser 1 and Laser 2 with both free-running and with Laser 1 locked to HDO. (b) Laser 2 is offset locked from Laser 1 (which is still PID locked to an HDO line) by 600 MHz. The standard deviation of the difference frequency is  $\sim 1$  MHz.

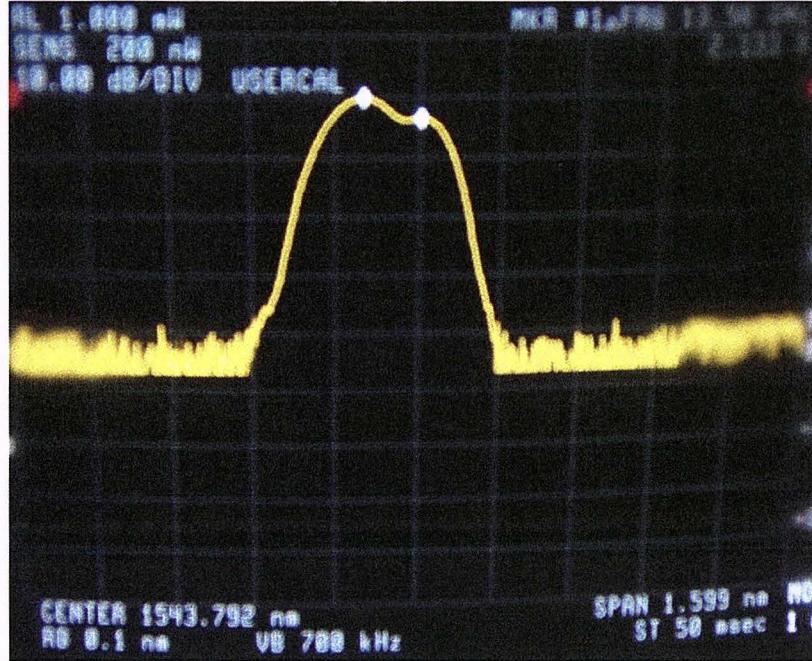


**Figure 7: Offset Locking.** Laser 2 (left peak) is offset locked to Laser 1 by 13.6 GHz.

#### 4. Analysis

The system demonstrated in this report was able to stabilize a diode laser to an absorption line of HDO with an accuracy of 20 kHz and a standard deviation linewidth of 3-4 MHz. Furthermore, another diode laser could be offset locked by any frequency from 10 Hz to  $\pm 20$  GHz with an accuracy of  $<300$  kHz and a standard deviation of  $\sim 1$  MHz. This  $\pm 20$  GHz range can easily be extended to  $\pm 40$  GHz (the bandwidth of our detector) with the present equipment; see Future Work for more details. Thus, Laser 2 can be locked to a known frequency to within 30 kHz and with a 5 MHz linewidth (in the worst case). Finally, the ability to continuously tune the difference between Laser 2 and Laser 3 over a broad range can be seen from Fig. 8. This figure was obtained by linearly sweeping the temperature of a diode laser from 23 to 35°C. Since 1 nm corresponds to about 125 GHz at 1550 nm, we see that the spacing of lines in this region is generally much less than 40 GHz.

Scanning would be accomplished by first locking Laser 1 to an HDO line then locking Laser 3 to another HDO line. Laser 2 could then be scanned from -40 GHz to +40 GHz from Laser 1. The difference between Lasers 2 and 3 give the final output. Then, Laser 3 would be moved to the next HDO line, and Laser 2 would be scanned again over the  $\pm 40$  GHz range. Table 2 details all of the high-intensity HDO peaks from 1537 to 1563 nm [24] and lists the

spacing between them in gigahertz. If Laser 1 was locked and fixed to the first line to provide an absolute laboratory frequency standard, Laser 3 could simply be stepped down this list. Since we have a  $\pm 40$  GHz offset locking range for Laser 2, we can continuously cover a step size of 80 GHz. Because most step sizes are less than 80 GHz, we can tune almost continuously over a 3-THz-wide band with only a few breaks. Furthermore, these gaps can be filled by increasing the sensitivity and by stepping Laser 1 to a nearby HDO line as explained in Future Work.

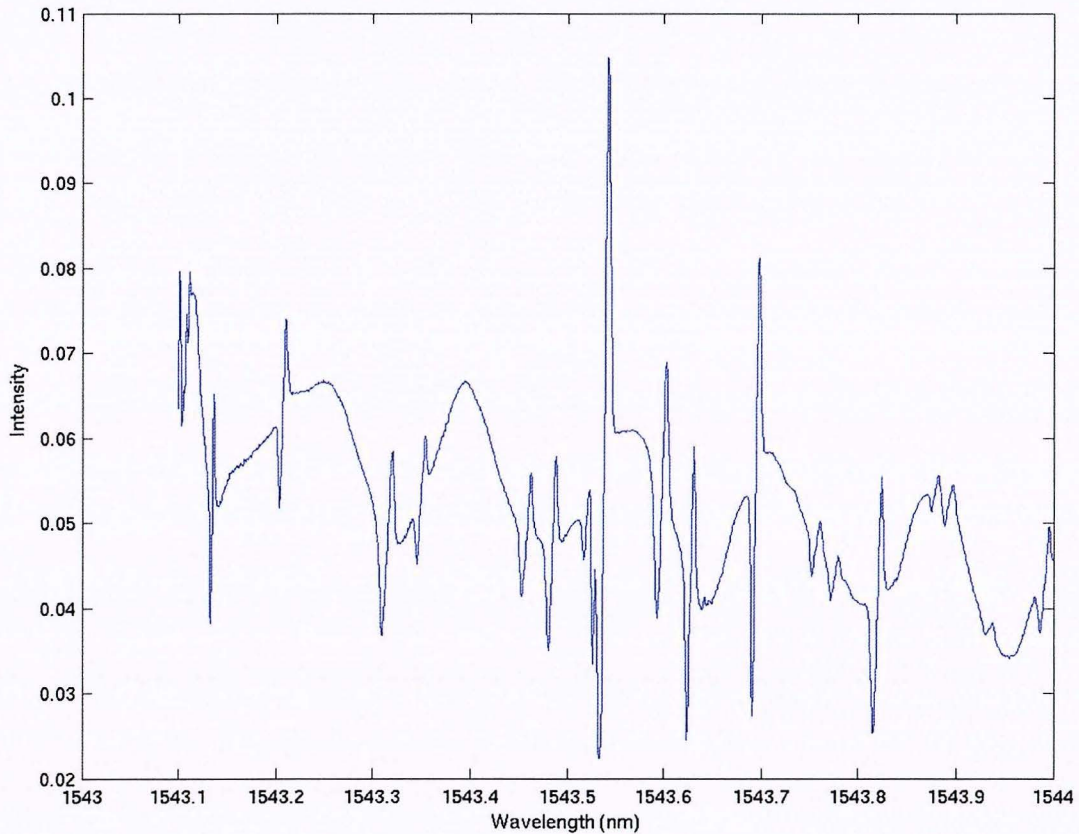


**Figure 8: HDO spectrum from 1543-1544 nm.** The spectrum was obtained by sweeping the temperature of a laser diode that was frequency modulated using current modulation. Notice the density of HDO in this region. Recent refinements have greatly reduced the etalons in the systems such that the HDO spectral lines can provide robust frequency stabilization signatures.

In generating spectra for comparison with SOFIA/Herschel data, the main requirement is for a broadly tunable, high-accuracy THz source. In this respect, the current setup works perfectly: Laser 2 has an accuracy of  $<300$  kHz and Laser 3 has an accuracy of  $\sim 20$  kHz, which means the difference is accurate to  $\sim 300$  kHz. Furthermore, the difference frequency should be

easily tunable over at least 3 THz (as demonstrated above) and most likely up to 15 THz (as discussed below). Finally, the linewidth of the difference should be  $\sim$ 7 MHz, which is about the same as many of the absorption linewidths of interested. While there are still many opportunities for improvement, this system is already good enough to be used for THz spectroscopy.

**Table 2: Primary line positions for HDO and frequency differences between adjacent lines.**

Line center (cm <sup>-1</sup> )	Line center (nm)	Δv (GHz)	Line center (cm <sup>-1</sup> )	Line center (nm)	Δv (GHz)
6397.06227	1563.217549		6464.40041	1546.933879	21.6081
6398.0647	1562.972628	30.0729	6464.5121	1546.907152	3.3507
6398.16229	1562.948789	2.9277	6466.43097	1546.448117	57.5661
6398.43773	1562.881507	8.2632	6467.19466	1546.265502	22.9107
6400.93916	1562.270747	75.0429	6467.37446	1546.222515	5.394
6405.03575	1561.271535	122.8977	6467.47541	1546.19838	3.0285
6406.59627	1560.891241	46.8156	6468.51489	1545.949908	31.1844
6411.509	1559.695229	147.3819	6470.68705	1545.430945	65.1648
6412.11458	1559.547927	18.1674	6470.75746	1545.414128	2.1123
6412.85512	1559.367834	22.2162	6474.7396	1544.463657	119.4642
6414.84056	1558.885199	59.5632	6475.52335	1544.276726	23.5125
6416.12346	1558.5735	38.487	6476.00252	1544.162463	14.3751
6417.56808	1558.222659	43.3386	6476.5363	1544.035197	16.0134
6420.9646	1557.398401	101.8956	6476.5797	1544.02485	1.302
6421.20138	1557.340972	7.1034	6476.9227	1543.943083	10.29
6425.91623	1556.198314	141.4455	6478.65266	1543.530812	51.8988
6430.86063	1555.001823	148.332	6479.0708	1543.431197	12.5442
6431.86827	1554.75821	30.2292	6479.8361	1543.24891	22.959
6434.31582	1554.166796	73.4265	6481.74926	1542.793403	57.3948
6436.39097	1553.665718	62.2545	6482.0913	1542.711995	10.2612
6438.53438	1553.148498	64.3023	6482.2846	1542.665992	5.799
6442.37	1552.223793	115.0686	6483.35655	1542.410929	32.1585
6444.61046	1551.684165	67.2138	6484.25468	1542.197291	26.9439
6444.95785	1551.600528	10.4217	6484.41333	1542.159559	4.7595
6445.1609	1551.551646	6.0915	6484.91848	1542.039431	15.1545
6446.6437	1551.194771	44.484	6485.007	1542.018382	2.6556
6447.63542	1550.95618	29.7516	6485.29679	1541.949478	8.6937
6448.04794	1550.856956	12.3756	6486.0405	1541.772673	22.3113
6449.22772	1550.573252	35.3934	6488.00439	1541.305985	58.9167
6450.88668	1550.174495	49.7688	6488.63351	1541.156545	18.8736
6451.54706	1550.015819	19.8114	6489.0009	1541.069288	11.0217
6452.17955	1549.863875	18.9747	6489.37283	1540.980964	11.1579
6453.71386	1549.495409	46.0293	6490.0348	1540.823787	19.8591
6455.241	1549.12884	45.8142	6491.923	1540.375633	56.646
6455.597	1549.043411	10.68	6491.97283	1540.36381	1.4949
6456.34939	1548.862894	22.5717	6492.67635	1540.196902	21.1056
6456.56845	1548.810344	6.5718	6493.95358	1539.893976	38.3169
6456.6974	1548.779412	3.8685	6494.45977	1539.773954	15.1857
6457.34076	1548.625103	19.3008	6494.67296	1539.72341	6.3957
6457.7669	1548.522911	12.7842	6495.318	1539.570503	19.3512
6458.5975	1548.323765	24.918	6495.346	1539.563866	0.84
6458.619	1548.318611	0.645	6495.567	1539.511485	6.63
6460.9164	1547.768053	68.922	6495.60222	1539.503138	1.0566
6461.6963	1547.581244	23.397	6496.62792	1539.260078	30.771
6462.2433	1547.450248	16.41	6499.29555	1538.62829	80.0289
6462.97911	1547.274071	22.0743	6500.6376	1538.310642	40.2615
6463.3702	1547.180448	11.7327	6501.79628	1538.036501	34.7604
6463.68014	1547.106259	9.2982	6502.3984	1537.894079	18.0636
			<b>Total change (GHz)</b>		<b>3160.0839</b>

## 5. Future work

This research was largely exploratory, and meant to determine whether the current lasers could be stabilized to the accuracy and linewidth required for THz photomixer spectroscopy applications. As currently demonstrated, the system has an offset tuning range of  $\pm 20$  GHz; however, we would like to extend this range to  $\pm 40$  GHz in order to ensure continuous tunability. Also, we used an RF synthesizer to provide the LO drive for the down-conversion. While this works, a complex and expensive RF synthesizer is overkill for this application. The modified system shown in Fig. 9 will provide  $\pm 40$  GHz of tuning without using an RF synthesizer. Briefly, a tunable YIG oscillator (Teledyne FS1001) generates RF from 2-10 GHz at 15 dBm. A switch allows the signal from the oscillator to be doubled with an active 3-13 GHz doubler (Miteq). This combination will provide a LO drive to the mixer of 2-20 GHz and 12-15 dBm. A Miteq even harmonic mixer then converts the 4-40 GHz RF input to an IF output of 0.1-1.5 GHz with a conversion loss of 9 dB. Since a harmonic mixer is used, only a 2-20 GHz LO is needed. With such a system, we will have a  $\pm 40$  GHz tuning range using only a 2-10 GHz RF source.

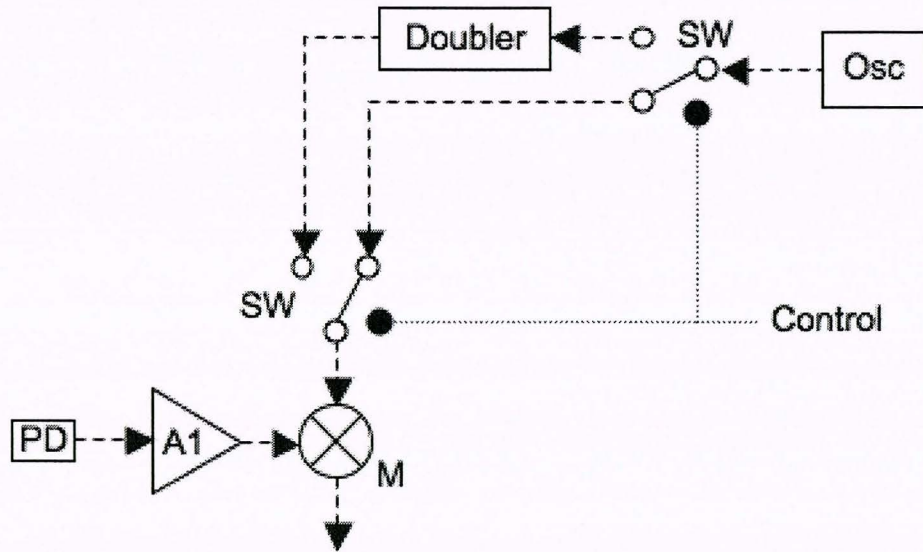


**Figure 9: Extending the offset locking capabilities to 40 GHz.** By using a 2-10 GHz YIG tuned oscillator (Osc) and an active doubler, we can produce RF at 13 dBm and between 2-20 GHz. We can then use this to drive an even-harmonic mixer, allowing conversion of RF (from the photodiode, PD, and wideband amplifier, A1) in the range of 4-40 GHz.

A difficulty noted earlier is that there are some breaks where the spacing between high intensity HDO lines is greater than 80 GHz. One solution to this problem is to use both Lasers 1 and 3 for broad ranging ‘step tuning.’ That is, Laser 1 can be locked to different HDO lines to allow for many more frequency difference possibilities between Lasers 1 and 3 than is possible by just tuning Laser 3. One drawback however, is that tuning both Lasers 1 and 3 is a bit more cumbersome for wide range scanning than just changing Laser 3. Another possibility is the use of a multi-pass absorption cell in the frequency stabilization setup. This would greatly increase the absorption signal-to-noise ratio (SNR), which would thus increase the sensitivity and allow locking to lower intensity lines. Furthermore, a multi-pass cell will also help to reduce noise in the locking loop, further improving the laser linewidth. Finally, as high speed photodetectors evolve scanning laser offset locks of  $>100$  GHz should be feasible in the near future.

Since the intrinsic short-term linewidths of the lasers are on the order of 100 kHz, our laser beat notes still have linewidths significantly higher than the intrinsic capabilities of the lasers themselves. Since we are planning on using this source to drive a THz Fabry-Perot cavity with mode spacing of about 1 GHz and cavity resonances some 10 MHz in width, the current linewidth is fine. As long as the average THz frequency over the cavity excitation time is constant and the linewidth is under 10 MHz, the radiation will only excite one cavity mode. Thus, the cavity will act like a filter. However, we would still like to reduce the linewidth for other possible applications in THz science such as the jet cooled spectroscopy of clusters and reactive intermediates in which the linewidths are sub-Doppler.

There are several possible reasons that the PID loop did not significantly reduce the short-term linewidth of the laser. One is a poorly tuned or noisy PID controller. We are going to try using a low-noise PID controller from Stanford Research Systems in the next round of tests and work on developing a tuning procedure. Another possible reason is that the feedback bandwidth may be too low: the laser fluctuations may be occurring faster than the controller can correct them or faster than the laser can change to correct them. With the new PID controller we will have 100 MHz of bandwidth; however, the feedback bandwidth could also be limited by the laser response speed. A solution to this problem is to use a fiber frequency shifter (acousto-optic modulator) to correct laser noise instead of relying on direct feedback to the laser, such as has been used to dramatically improve the phase noise performance of the laser-based LO scheme proposed for the Atacama Large Millimeter Array (ALMA) [25].

Another issue limiting the performance is any component of the noise error signal that is not due to laser fluctuations. Increasing the SNR with an amplifier seemed to help; however, since the amplifier was not running at saturation a significant amount of the 1550 nm light may have been due to Amplified Spontaneous Emission, or ASE. To reduce the amplifier noise we need to run the amplifier at full power, split the output, and send a small portion of it to the FMS locking setup. The addition of a multi-pass HDO cell will also greatly improve the SNR. We are also looking at low-noise detectors/preamps including possibly liquid nitrogen cooled detectors. By adding other species to the absorption cell, such as C<sub>2</sub>H<sub>2</sub>, which absorb at slightly longer or shorter wavelengths than does HDO, the tuning range of the THz spectrometer can be extended to cover the full telecommunications bands from 1520 to 1640 nm (or nearly 15 THz).

Finally, we are considering use a two step locking system employing the current method for the coarse locking loop and then including a fine locking loop using saturated absorption spectroscopy [11, 26]. Saturated absorption techniques work by eliminating Doppler broadening through the selection of the subset of atoms or molecules in the sample whose velocities are perpendicular to the propagation axis of the radiation. This produces a much narrow absorption band (~5 MHz instead of ~600 MHz), which thus allows greater locking sensitivity, but at the cost of signal sensitivity since only a small fraction of the sample contributes to the signal. When the photomixers are operational, it should also be possible to use well calibrated THz lines (such as those from CO or SO<sub>2</sub>) whose Doppler widths are only a few MHz to measure the combination differences between line pairs at 1550 nm to high precision.

## 6. Conclusion

We have demonstrated the ability to combine two laser beams, which are offset from each other by any frequency up to at least 3 THz. Furthermore, both of these lasers are stabilized to a 3-5 MHz linewidth and provide up to 1 W of optical power with amplification. By combining this system with ultra-high-speed photomixers, we can generate broadly tunable radiation up to at least 3 THz with a linewidth of less than 10 MHz and an accuracy over 2 hours of ~300 kHz. In addition, we have proposed methods of reducing the linewidth even further, hopefully to 1 MHz. The present system is based on HDO, but by choosing various gases offsets up to 15 THz should be feasible. Because the system is fiber-based, the spatial mode patterns of the two

frequencies are inherently the same, which should lead to efficient THz generation in traveling wave photomixers.

To our knowledge there has been no other demonstration of a tunable source with this bandwidth capability and ease of tunability. Another major advantage of this system is its simplicity. All that is needed to generate any desired output frequency is to identify two molecular lines that are separated by the approximate frequency desired (which is easily done with simple computer software), set these two lasers to the desired wavelengths and engage the PID loops, and then choose the desired offset frequency. Overall, this system shows great promise for becoming a readily accessible source of broadly tunable, narrow linewidth, and high accuracy THz radiation.

## References

1. Blake, G.A., *Microwave and THz Spectroscopy*, in *Encyclopedia of Chemical Physics and Physical Chemistry*, N.S. J. Moore, Editor. 2000, Institute of Physics Publ.: Bristol. p. 31-44.
2. Williams, B.S. et al. 2006, *High Power THz Quantum Cascade Lasers*, Elec. Lett. 42, p. 89-91.
3. Braakman, R., *Laboratory and astronomical studies of the THz spectra of amino acids*. Candidacy report, 2005, California Institute of Technology.
4. Chen, P., et al., *Spectroscopic applications and frequency locking of THz photomixing with distributed-Bragg-reflector diode lasers in low-temperature-grown GaAs*. Applied Physics Letters, 1997. 71(12): p. 1601-1603.
5. Matsuura, S., et al., *A tunable cavity-locked diode laser source for terahertz photomixing*. IEEE Transactions on Microwave Theory and Techniques, 2000. 48(3): p. 380-387.
6. Pin, C., et al. *A three-diode-laser, terahertz-difference-frequency synthesizer and its applications toward far-infrared spectroscopy of ammonia and water*. 2000.
7. Bowring, N.J., D. Li, and J.G. Baker, *Frequency Stabilization of a  $0.78\mu\text{m}$  GaAlAs Laser-diode to Acetylene Absorption-lines*. Measurement Science & Technology, 1994. 5(10): p. 1313-1316.
8. Bradley, C.C., J. Chen, and R.G. Hulet, *Instrumentation for the Stable Operation of Laser-diodes*. Review of Scientific Instruments, 1990. 61(8): p. 2097-2101.
9. Bruner, A., et al., *Frequency stabilization of a diode laser at 1540 nm by locking to sub-Doppler lines of potassium at 770 nm*. Applied Optics, 1998. 37(6): p. 1049-1052.
10. Bruner, A., et al., *Frequency stability at the kilohertz level of a rubidium-locked diode laser at 192.114 THz*. Applied Optics, 1998. 37(27): p. 6410-6414.
11. Hall, J.L., *Frequency-stabilized Lasers - From the Beginning Toward the Future*. Laser Physics, 1994. 4(2): p. 306-318.
12. Lee, W.D., et al., *Frequency Stabilization of an External-cavity Diode-laser*. Applied Physics Letters, 1990. 57(21): p. 2181-2183.
13. Ludvigsen, H. and C. Holmlund, *Frequency Stabilization of a GaAlAs Semiconductor-laser to an Absorption-line of Iodine Vapor*. Review of Scientific Instruments, 1992. 63(4): p. 2135-2137.
14. Ray, A., et al., *Frequency stabilisation of a GaAlAs semiconductor diode laser to an absorption line of water vapour at 822 nm*. IEE Proceedings-Optoelectronics, 2004. 151(6): p. 490-495.

15. Weel, M. and A. Kumarakrishnan, *Laser-frequency stabilization using a lock-in amplifier*. Canadian Journal of Physics, 2002. 80(12): p. 1449-1458.
16. Wieman, C.E. and L. Hollberg, *Using Diode-lasers for Atomic Physics*. Review of Scientific Instruments, 1991. 62(1): p. 1-20.
17. Yanagawa, T., et al., *Frequency Stabilization of an InGaAsP Distributed Feedback Laser to an NH<sub>3</sub> Absorption-line at 15137Å with an External Frequency Modulator*. Applied Physics Letters, 1985. 47(10): p. 1036-1038.
18. Hall, G.E. and S.W. North, *Transient laser frequency modulation spectroscopy*. Annual Review of Physical Chemistry, 2000. 51: p. 243-274.
19. *PID Controller*. [cited 1 May 2007]; Available from: [http://en.wikipedia.org/wiki/PID\\_controller](http://en.wikipedia.org/wiki/PID_controller).
20. Matsuura, S., et al., *Design and characterization of optical-THz phase-matched traveling-wave photomixers*. Proceedings of the SPIE - The International Society for Optical Engineering, 1999. 3795: p. 484-492.
21. Matsuura, S., et al., *A traveling-wave THz photomixer based on angle-tuned phase matching*. Applied Physics Letters, 1999. 74(19): p. 2872-2874.
22. Matsuura, S. and H. Ito, *Generation of CW terahertz radiation with photomixing*, in *Terahertz Optoelectronics*. 2005. p. 157-202.
23. Sukhotin, M., et al., *Photomixing and photoconductor measurements on ErAs/InGaAs at 1.55  $\mu$ m*. Applied Physics Letters, 2003. 82(18): p. 3116-3118.
24. Toth, R.A., *Line positions and strengths of HDO between 6000 and 7700 cm<sup>-1</sup>*. Journal of Molecular Spectroscopy, 1997. 186(1): p. 66-89.
25. Shillue, B. and L. D'Addario, *A New Configuration for the ALMA Laser Synthesizer*. ALMA Memo #484. 2004-06-17.
26. Hall, J.L., et al., *Optical Heterodyne Saturation Spectroscopy*. Applied Physics Letters, 1981. 39(9): p. 680-682.